Monthly Notices
of the
ROYAL ASTRONOMICAL SOCIETY

Mon. Not. R. Astron. Soc. **410,** 2497–2505 (2011) doi:10.1111/j.1365-2966.2010.17628.x

Multistate observations of the Galactic black hole XTE J1752−223: evidence for an intermediate black hole spin

R. C. Reis,[1⋆] J. M. Miller,[2] A. C. Fabian,[1] E. M. Cackett,[2] D. Maitra,[2] C. S. Reynolds,[3,4] M. Rupen,[5] D. T. H. Steeghs[6] and R. Wijnands[7]

[1]*Institute of Astronomy, Madingley Road, Cambridge CB3 0HA*
[2]*Department of Astronomy, University of Michigan, 500 Church Street, Ann Arbor, MI 48109, USA*
[3]*Department of Astronomy, University of Maryland, College Park, MD 20742, USA*
[4]*Joint Space Science Institute (JSI), University of Maryland, College Park, MD 20742, USA*
[5]*NRAO, Array Operations Center, 1003 Lopezville Road, Socorro, NM 87801, USA*
[6]*Department of Physics, University of Warwick, Coventry CV4 7AL*
[7]*Astronomical Institute 'Anton Pannekoek', University of Amsterdam, Postbus 94249, 1090 GE Amsterdam, the Netherlands*

Accepted 2010 September 1. Received 2010 August 16; in original form 2010 June 27

ABSTRACT

The Galactic black hole candidate XTE J1752−223 was observed during the decay of its 2009 outburst with the *Suzaku* and *XMM–Newton* observatories. The observed spectra are consistent with the source being in the 'intermediate' and 'low-hard' states, respectively. The presence of a strong, relativistic iron emission line is clearly detected in both observations and the line profiles are found to be remarkably consistent and robust to a variety of continuum models. This strongly points to the compact object in XTE J1752−223 being a stellar mass black hole accretor and not a neutron star. Physically motivated and self-consistent reflection models for the Fe Kα emission-line profile and disc reflection spectrum rule out either a non-rotating, Schwarzschild black hole or a maximally rotating, Kerr black hole at greater than 3σ level of confidence. Using a fully relativistic line function in which the black hole spin parameter is a variable, we have formally constrained the spin parameter to be $0.52 \pm 0.11(1\sigma)$. Furthermore, we show that the source in the low-hard state still requires an optically thick disc component having a luminosity which is consistent with the $L \propto T^4$ relation expected for a thin disc extending down to the innermost stable circular orbit. Our result is in contrast to the prevailing paradigm that the disc is truncated in the low-hard state.

Key words: accretion, accretion discs – black hole physics – line: profiles – relativistic processes – X-rays: binaries – X-rays: individual: XTE J1752–223.

1 INTRODUCTION

Stellar mass Galactic black holes in X-ray binaries represent nearby laboratories in which the inner regions of the accretion flow can be studied in detail, thus providing information on both the geometry of the accretion disc and on intrinsic physical parameters such as black hole mass and spin. Whereas the supermassive black holes that power active galactic nuclei (AGNs) are variable by a factor of several, the mass accretion rate on to a stellar mass black hole can vary by 10^8 between quiescence and outburst peak. This affords unique opportunities to study how accretion flows evolve, including how relativistic jets are produced and quenched (Fender, Belloni & Gallo 2004). At relatively high mass accretion rates, where a standard Shakura & Sunyaev (1973) accretion disc remains at the innermost stable circular orbit (ISCO), the X-ray spectrum of these sources permit constraints on black hole spin parameters (e.g. Miller et al. 2002; McClintock et al. 2006; Shafee et al. 2006; Reis et al. 2008; Miller et al. 2009a).

Presently, dynamical constraints demand a black hole primary in 20 sources in the Milky Way and Large Magellanic Cloud (Remillard & McClintock 2006). In approximately twice this number of sources, observing constraints have prevented dynamical constraints on the mass of the primary, but X-ray spectra, timing and multiwavelength properties clearly indicate that the binary harbours a black hole. These sources are often called 'black hole candidates' (Remillard & McClintock 2006). New candidate black hole transients that are found to lie in favourable fields and to not suffer excessive extinction – candidates that will permit dynamical constraints via radial velocity curves – are especially important sources.

XTE J1752−223 was discovered during periodic *RXTE* scans of the Galactic bulge region on 2009 October 23 (Markwardt et al. 2009a). Observations with the *Swift*/BAT and *MAXI*/GSC soon confirmed the new source (Markwardt et al. 2009b; Nakahira et al. 2009,

⋆E-mail: rcr36@ast.cam.ac.uk

2010). Additional prompt observations failed to detect pulsations; the absence of pulsations and the nature of the spectrum led to an early identification of XTE J1752−223 as a new black hole candidate (Markwardt et al. 2009b). Many black hole X-ray binaries begin their rise to outburst peak in the 'low/hard' state, in which jet emission is typical (Remillard & McClintock 2006); prompt radio observations of XTE J1752−223 with *ATCA* detected a flat-spectrum radio sources, consistent with emission from a compact jet (Brocksopp et al. 2009). Also typical of black holes, XTE J1725−223 was detected in hard X-rays with the *Fermi*/GBM (Wilson-Hodge et al. 2009). A bright optical counterpart has been reported (Torres et al. 2009a), together with the presence of a broad Hα emission line (Torres et al. 2009b). The column density along the line of sight to XTE J1752−223 is modest (4.5×10^{21} cm^{-2}, Dickey & Lockman 1990), and a dynamical mass constraint may be possible.

Understanding the role of black hole spin in shaping accretion flows on to – and jets from – black holes is an important and timely aim. The dimensionless spin parameter of a black hole is given by $a = cJ/GM^2$, where J is angular momentum, G is Newton's constant and M is the mass of the black hole. In the case of stellar mass black holes, the spin parameter cannot be changed significantly through the limited mass that can be accreted from the companion star (Thorne 1974; Gammie, Shapiro & McKinney 2004). Thus, the spin of black holes in X-ray binaries is set by the creation event, likely a gamma-ray burst (GRB) or supernova (SN).

The mass of the black hole in XTE J1752−223 and the distance to this source are not presently known, but modelling of relativistic Fe K disc lines – as well as all other associated reflection features – in the spectra of X-ray binaries, can constrain spin parameters without these quantities (e.g. Martocchia et al. 2002; Miller et al. 2002, 2004a, 2009a; Reis et al. 2008, 2009a). The reflection component arise as hard emission from the corona irradiates the cooler disc and results in 'reflection signatures' consisting of fluorescent and recombination emission lines as well as absorption features (Ross & Fabian 2005). The most prominent of these signatures being the broad, skewed Fe Kα line. Constraint on the spin parameter arises because the Doppler shifts and gravitational redshifts that shape such lines depend only on the relative depth of the disc within the potential well, not on an absolute quantity. When the mass and distance to a source are known, modelling of the accretion disc continuum can give a completely independent spin constraint (e.g. McClintock et al. 2006; Gou et al. 2009).

In this paper, we draw on observations of XTE J1752−223 with *XMM–Newton* and *Suzaku* to constrain the nature of the innermost accretion flow in this source, and to constrain the spin parameter of the black hole. The observations were made at very different points during the current outburst of XTE J1752−223: *Suzaku* observed the source in an 'intermediate' state, while *XMM–Newton* observed the source in a 'low/hard' state. A relativistic iron disc line is detected in both observations; the profile is remarkably consistent between the two.

2 DATA REDUCTION

XTE J1752−223 was observed during the decay of its 2009 outburst with *Suzaku* (Mitsuda et al. 2007) on February 24 (hereafter Obs. 1), and subsequently with *XMM–Newton* (Jansen et al. 2001) on April 6 (hereafter Obs. 2) for a total exposure of approximately 42 ks each time. The *Suzaku* observation caught the source in the intermediate state during its decay from maximum flux as shown in Fig. 1 . At

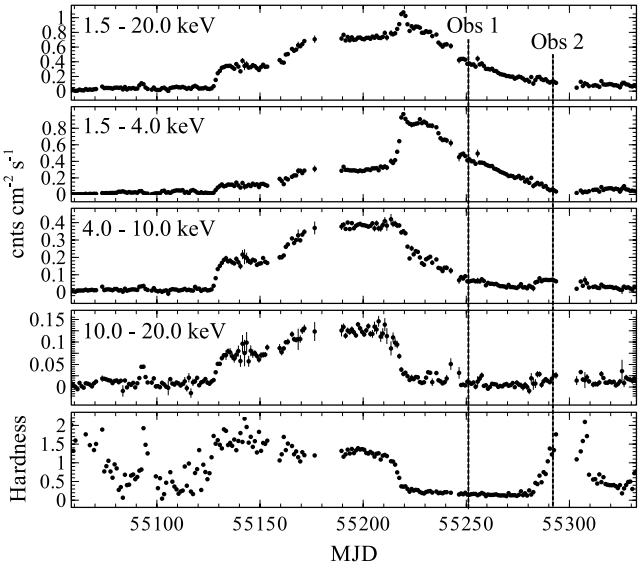

Figure 1. MAXI light curve for XTE J1752−223 in four energy bins and hardness ratio (bottom panel) defined as the ratio between the 4–10 and 1.5–4 keV energy range. The dotted vertical lines shows the time for the *Suzaku* (Obs. 1) and *XMM–Newton* (Obs. 2) observations presented in this paper. It is clear that the source was observed in two different spectral states.

the time of the *XMM–Newton* observation, XTE J1752−223 was back in the low-hard state.

The three operating detectors constituting the X-ray Imaging Spectrometer (XIS; Koyama et al. 2007) onboard of *Suzaku* were operated in the 'burst' mode with the front-illuminated (FI; XIS0 and 3) and back-illuminated (BI; XIS1) detectors in the 2×2 and 3×3 editing modes, respectively. The observation resulted in a total (co-added) good exposure of approximately 12.2 ks and 516 s for the FI and BI instruments, respectively. Due to the short exposure time of the BI camera, throughout this paper we will only discuss the results obtained with the FI instrument. Using the latest HEASOFT v6.9 software package we processed the unfiltered event files for each of the two remaining CCDs following the *Suzaku* Data Reduction Guide.[1] New attitude files were created using the AEATTCOR script[2] (Uchiyama et al. 2008) in order to correct for shift in the mean position of the source caused by the wobbling of the optical axis. The FTOOL xiscoord was used to create new event files which were then further corrected by rerunning the *Suzaku* pipeline with the latest calibration, as well as the associated screening criteria files. The good time intervals provided by the XIS team were employed in all cases to exclude any possible telemetry saturations. XSELECT was used to extract spectral products from these event files. Source events were extracted from a square-annulus region with inner and outer width of 30 and 240 arcsec, respectively, and background spectra from another region of the same size, devoid of any obvious contaminating emission, elsewhere on the same chip. The script 'xisresp'[3] with the 'medium' input was used to obtain individual ancillary response files (arfs) and redistribution matrix files (rmfs). 'xisresp' calls the tools 'xisrmfgen' and 'xissimarfgen'. Finally, we combined the spectra and response files from the two front-illuminated instruments (XIS0 and XIS3) using the FTOOL addascaspec to increase signal-to-noise ratio. The FTOOL grppha was used to give at least 100 counts per spectral bin. The Hard X-ray

[1] http://heasarc.gsfc.nasa.gov/docs/suzaku/analysis/
[2] http://space.mit.edu/cxc/software/suzaku/aeatt.html
[3] http://suzaku.gsfc.nasa.gov/docs/suzaku/analysis/xisresp

Detector (HXD; Takahashi et al. 2007) was operated in the normal mode. The appropriate response and tuned non-X-ray background (NXB) files for HXD nominal pointing were downloaded[4] and the data were reprocessed in accordance with the *Suzaku* Data Reduction Guide. Common good time intervals were obtained with MGTIME which combines the good times of the event and background files, and XSELECT was used to extract spectral products. Dead time corrections were applied with HXDDTCOR, and the exposures of the NXB spectra were increased by a factor of 10, as instructed by the data reduction guide. The contribution from the cosmic X-ray background (CXB) was simulated using the form of Boldt (1987), with the appropriate normalization for the HXD nominal pointing, resulting in a CXB rate of 0.021 count s^{-1}. The NXB and CXB spectra were then combined using MATHPHA to give a total background spectrum, to which a 2 per cent systematic uncertainty was added. The source spectrum was finally grouped to at least 500 counts per spectral bin.

The EPIC-pn camera (Strüder et al. 2001) onboard *XMM–Newton* was operated in 'timing' mode with a 'medium' optical blocking filter. The EPIC-MOS1 and EPIC-MOS2 cameras (Turner et al. 2001) were operated in the 'imaging' mode. Starting with the unscreened level 1 data files, we generated concatenated and calibrated event lists for the different instruments using the latest *XMM–Newton* Science Analysis System v 10.0.0 (SAS). EPIC-pn events were extracted from a stripe in RAWX (30–48) versus RAWY (2.5–199.5) space. Bad pixels and events too close to chip edges were ignored by requiring 'FLAG = 0' and 'PATTERN $\leqslant$ 4'. The energy channels were initially binned by a factor of 5 to create a spectrum. The EPIC-MOS data suffered heavily from pile-up and will therefore not be included in the forthcoming analysis. We used the SAS task epatplot to assess the level of pile-up in the EPIC-pn spectrum and found it to be insignificant. The EPIC-pn count rate is approximately 150 count s^{-1} which is well below the nominal pile-up limit for the instrument in timing mode ($\approx$800 count s^{-1}). Response files were created in the standard way using the tools rmfgen and arfgen. The total good exposure time selected was 1.8 ks. Because of the high source flux in the EPIC-pn spectrum we did not subtract any background. Finally we rebinned the spectrum with the tool pharbn,[5] to have three energy channels per resolution element, and at least 20 counts per channel. Throughout this paper XIS-FI and EPIC-pn spectra are fitted in the 1.3–10.0 keV energy range, respectively. This lower limit was chosen as it was found that the data below this energy showed strong positive residuals above any reasonable continuum. Similar residuals were reported by Hiemstra et al. (2010) based on an EPIC-pn-timing observation of XTE J1652−453 where the authors associated it with possible calibration issues related with the redistribution matrix of the timing-mode data. The PIN spectrum is restricted to the 20.0–45.0 keV energy range and fit simultaneously with the XIS data by adding a normalization factor of 1.18 with respect to that of the FI spectrum. All errors reported in this work are 90 per cent confidence errors obtained by allowing all parameters to vary, unless otherwise noted.

3 DATA ANALYSES AND RESULTS

3.1 Phenomenological models

The X-ray spectrum of stellar mass black hole binaries can usually be phenomenologically characterized by a continuum consisting of an absorbed power law together with a thermal disc-blackbody component. In addition to this continuum, often there is also a broad emission line at ∼6.4 keV (see e.g. Miller 2007). Anticipating a similar combination for the continuum of XTE J1752−223, we start by fitting the energy range 1.3–4.5 and 8.0–45.0 keV with a power law modified by interstellar absorption (PHABS[6] model in XSPEC) together with the disc blackbody model DISKBB (Mitsuda et al. 1984; Makishima et al. 1986). Initially we constrain the neutral-hydrogen column density ($N_{\rm H}$) to be the same between the two observations. The model parameters are thus the (global) $N_{\rm H}$, as well as disc temperatures ($T_{\rm disc}$), power-law indices (Γ) and normalizations (N) for each observation. This combination resulted in a good description of the continuum, with the bulk of the residuals coming from the energy range between 1.7 and 2.5 keV possibly due to the Au M-shell edges and Si features in the detectors. Hereafter this energy range will be ignored. The resulting fit gives $\chi^2/\nu = 2121.5/1282$ with a disc temperature of 0.570 ± 0.002 and 0.287 ± 0.004 keV for Obs. 1 and 2, respectively. The total, luminosity in the 0.5–10 keV range, (L_T) is $L_{T1} \simeq 2.5(d/10\,{\rm kpc}) \times 10^{38}\,{\rm erg\,s^{-1}}$ and $L_{T2} \simeq 3.0(d/10\,{\rm kpc}) \times 10^{37}\,{\rm erg\,s^{-1}}$ for Obs. 1 and 2, respectively. Assuming a fiducial black hole of $10\,{\rm M}_\odot$ at a distance of 10 kpc places our observations at $L/L_{\rm Edd} \simeq 0.2$ and 0.02, respectively. The latter value for the luminosity state of XTE J1752−223 during the *XMM–Newton* observation is over an order of magnitude higher than the range explored by Tomsick et al. (2009) for GX 339−4 (0.14 per cent $L_{\rm Edd}$), where the authors presented the first direct evidence for the truncation of the accretion disc in the low-hard state of accreting black holes.

The unabsorbed disc flux decreases from $(2.57 \pm 0.02) \times 10^{-8}\,{\rm erg\,cm^{-2}\,s^{-1}}$ in Obs. 1 to $(1.71 \pm 0.07) \times 10^{-9}\,{\rm erg\,cm^{-2}\,s^{-1}}$ in Obs. 2 so that $(T_1/T_2)^4 = 17.7 \pm 1.0$ and $F_1/F_2 = 15.0 \pm 1.0$ which is remarkably consistent with the $L \propto T^4$ relation expected for a standard thin accretion disc extending down to the ISCO (see e.g. Frank, King & Raine 2002) in both spectral states.

The total neutral hydrogen column density in the line of sight to low-mass X-ray binaries is not expected to vary at the time-scales considered here (Miller, Cackett & Reis 2009b). However, due to the uncertainties in the cross calibration between the instruments we hereafter allow this parameter to differ between the *Suzaku* and *XMM–Newton* observations in order to obtain a better description of the continuum. Fig. 2 shows the data/model ratio for the two observations of XTE J1752−223 fitted with a variety of plausible continuum models over the full energy range allowed for each spectrum excepting the iron K band between 4.5–8.0 keV. The models used for the continua are listed in Table 1. Model 2 replaces the power-law component in Model 1 with the thermal Comptonization code, COMPTT, of Titarchuk (1994) where the input seed photon temperature (kT_0) was tied to the thermal disc temperature modelled with DISKBB. The temperature (KT_e) and optical depth (τ) of the plasma are further free parameters of this model. As a further test to the robustness of the line profile we replaced in Model 3 the COMPTT component with COMPPS (Poutanen & Svensson 1996) which is better suited for high electron temperatures. It is clear from Fig. 2 and Table 1 that the extent and overall shape of the line does not strongly depend on the chosen continuum.

Allowing the neutral hydrogen column density to differ between the observations resulted in a higher disc temperature and lower $N_{\rm H}$ for the second observation as compared to the results presented

[4] http://www.astro.isas.ac.jp/suzaku/analysis/hxd/

[5] http://virgo.bitp.kiev.ua/docs/xmm_sas/Pawel/reduction/pharbn

[6] Using the standard BCMC cross-sections (Balucinska-Church & McCammon 1992) and ANGR abundances (Anders & Grevesse 1989).

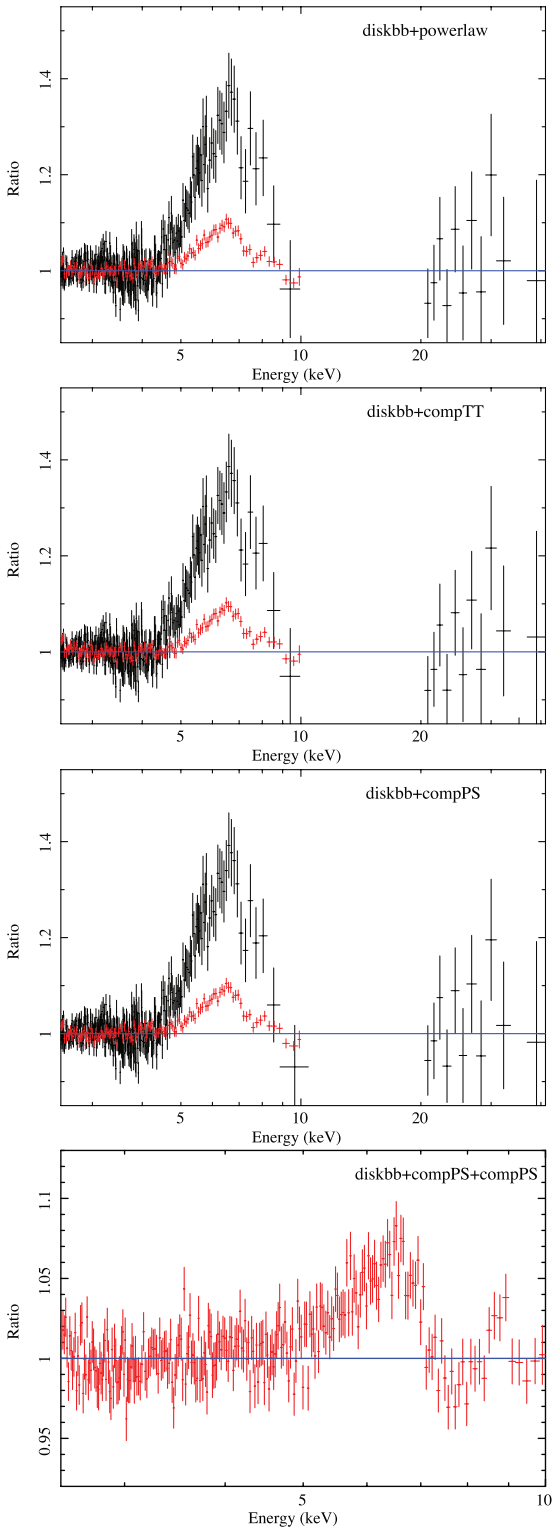

Figure 2. Data/model ratio to a variety of absorbed Compton components together with thermal disc emission. *Suzaku* spectra (XIS and PIN) for the 2010 February observation are shown in black. The *XMM–Newton* (EPIC-pn) 2010 April spectrum is shown in red. The XIS and EPIC-pn data were fitted in the 1.3–4.5 and 8.0–10.0 keV energy range. The PIN data were fitted between 20.0 and −45.0 keV. The bottom panel shows the double Compton model applied to the low-hard state data only. The residuals show that a broad iron emission line extending to approximately 4 keV is present in both observations independent of the model used for the hard emission. The data have been rebinned for plotting purposes.

above. Although this fit yields an improvement in χ^2 it is unlikely that such a large variation in $N_{\rm H}$ is real and the accompanying high temperature is merely a response to the low $N_{\rm H}$. We remind the reader that the purpose of these phenomenological models is simply to highlight the robustness of the line profile to a variety of – very different – continua. From Table 1 we see that the strength of the line – characterized by its equivalent width (EW) – for Obs. 1 (Obs. 2) does not depend on the curvature of the continuum, with a value of approximately 270(180) eV for the least curved model (Model 1) and 290 (170) eV for the highly curved Comptonization model COMPPS (Model 3).

We again see from Fig. 3 that the shape of the line profile does not vary significantly during the two observations even though we are looking at two distinct states of XTE J1752−223 (see Fig. 1). Such a line profile is usually attributed to gravitational effects close to the central regions of a black hole (Fabian et al. 1989; Laor 1991). Alternative explanations such as Comptonization, velocity shifts and/or scattering effects have been shown to be extremely unlikely source of line broadening (e.g. Fabian et al. 1995; Reynolds & Wilms 2000; Miller et al. 2004b, see also Hiemstra et al. 2010). We therefore proceed by assuming a relativistic origin for the broad emission line and as such begin by modelling the residuals seen in Fig. 2 with the the LAOR model (Laor 1991). This model describes a broad line emerging from an accretion disc with emissivity profile described by a power law of the form $\epsilon_{(r)} = r^{-q}$ and an inner radius $r_{\rm in}$ in units of $r_{\rm g} = GM/c^2$. The outer disc radius was fixed at the maximum allowed value of $400r_{\rm g}$. Only the inner radius and disc inclination, i were tied between the observations.

When we fit the line profile with a model such as LAOR, together with a separate disc component (e.g. Model 1) we find a degeneracy between the emissivity index (q) and the inclination of the system. The inclination as such is determined from the blue wing of the line profile and in XTE J1752−223 this region is coincidental with the downturn of the disc emission. Fig. 4 shows the emissivity index[7] versus inclination parameter space for Model 1. It is apparent that there are two set of solutions: (i) disc inclination $i \lesssim 50^\circ$ with $3 \lesssim q \lesssim 5$ and (ii) $i > 50^\circ$ with $q > 5$. We will proceed with the rest of this analysis by confining the inclination to be less than 40° and $q < 5.5$ thus being consistent with values for emissivities found in the literature (see e.g. Miller 2007) and adhering to the value of 3 expected for a standard accretion disc (Reynolds & Nowak 2003). It should also be said that we do not expect the inclination of this system to be high based on both the lack of dips and absorption – as expected for edge-on systems – as well as the lack of high-frequency QPOs. Furthermore, we will show in the following section that this degeneracy is indeed broken when we fit the data with a self-consistent reflection model that also incorporates the thermal emission. Table 1 details the various parameters found for the three continuum models together with the LAOR line profile. In all cases we find a strong relativistic line with an inner radius of approximately $4r_{\rm g}$. In order further to address the question of whether the edge of the inner disc recedes between the two states we allowed in Model 1b for $r_{\rm in}$ to vary between the observations. Fig. 5 shows the contour map for these two values. It is clear that in *both* states the inner-edge of the accretion disc in XTE J1752−223 extends down to approximately $4r_{\rm g}$, with such a value

[7] We are only showing the emissivity index for Obs. 1 versus inclination; however, a similar degeneracy is also found for q in Obs. 2.

Table 1. Joint fits with simple phenomenological models.

	Model 1 diskbb+power law		Model 1b diskbb+power law		Model 2 diskbb+compTT		Model 3 diskbb+compPS	
Parameters	Obs. 1	Obs. 2	Obs. 1	Obs. 2	Obs. 1	Obs. 2	Obs. 1	Obs. 2
$N_{\rm H}$ ($\times 10^{22}$ cm^{-2})	0.56 ± 0.01	0.14 ± 0.02	0.563 ± 0.005	0.134 ± 0.005	$0.551^{+0.009}_{-0.004}$	$0.15(f)$	$0.550^{+0.008}_{-0.004}$	0.07 ± 0.01
$T_{\rm disc}$(keV)	$0.561^{+0.002}_{-0.001}$	$0.42^{+0.02}_{-0.01}$	$0.561^{+0.005}_{-0.001}$	$0.429^{+0.010}_{-0.004}$	$0.560^{+0.001}_{-0.002}$	$0.336^{+0.004}_{-0.005}$	0.563 ± 0.002	0.434 ± 0.001
Γ	$2.57^{+0.06}_{-0.05}$	1.82 ± 0.01	$2.52^{+0.03}_{-0.05}$	1.82 ± 0.01	–	–	–	–
kT_0 (keV)	–	–	–	–	$0.560^{+0.001}_{-0.002}$	$0.336^{+0.004}_{-0.005}$	0.563 ± 0.002	0.434 ± 0.001
kT_e (keV)	–	–	–	–	96^{+160}_{-60}	32^{+98}_{-14}	101^{+39}_{-36}	27^{+98}_{-14}
τ	–	–	–	–	$0.1^{+0.8}_{-0.1}$	$1.2^{+0.7}_{-0.5}$	$0.3^{+0.7}_{-0.2}$	$3.0_{-0.8}$
$E_{\rm Laor}$ (keV)	$6.91^{+0.06}_{-0.21}$	$6.97_{-0.03}$	$6.97_{-0.23}$	$6.97_{-0.01}$	$6.84^{+0.17}_{-0.20}$	$6.97_{-0.02}$	$6.93^{+0.04}_{-0.22}$	$6.97_{-0.04}$
EW (ev)	270^{+70}_{-50}	180 ± 20	280^{+50}_{-40}	190 ± 20	250 ± 50	150 ± 10	290 ± 60	170^{+30}_{-10}
q	4.2 ± 0.5	$3.3^{+0.3}_{-0.1}$	4.6 ± 0.4	3.9 ± 0.3	$4.2^{+0.9}_{-0.5}$	3.2 ± 0.1	$4.3^{+0.5}_{-0.4}$	3.2 ± 0.1
i (°)	19^{+7}_{-3}	=Obs. 1	28 ± 2	=Obs. 1	16^{+3}_{-6}	=Obs. 1	18^{+5}_{-3}	=Obs. 1
$r_{\rm in}$ ($r_{\rm g}$)	$4.1^{+0.3}_{-0.6}$	=Obs. 1	$2.8^{+0.3}_{-0.1}$	3.9 ± 0.5	4.9 ± 0.5	=Obs. 1	4.0 ± 0.4	=Obs. 1
χ^2/ν	2645.4/2247		2634.9/2246		2672.0/2246		2626.7/2245	

Note: Results of joint *Suzaku* (Obs. 1) and *XMM–Newton* (Obs. 2) fits with simple continuum models. In all cases the inclination and inner disc radii were tied between the observations and the disc component was modelled with the standard multicolour disc model DISKBB (Mitsuda et al. 1984). The hard continuum in Model 1 is assumed to consist of a simple power law. Models 2 and 3 replaces the power law with the Comptonization codes of Titarchuk (1994) and Poutanen & Svensson (1996), respectively. In both cases the input photon temperature (kT_0) were tied to the thermal disc temperature. For Model 2 a disc geometry was assumed and the column density in Obs. 2 was frozen at the value found in Model 1 so as to prevent it from going to zero. In Model 3 we assume that the Compton cloud has a spherical geometry (parameter 4) and deactivated the reflection option. All errors are 90 per cent confidence.

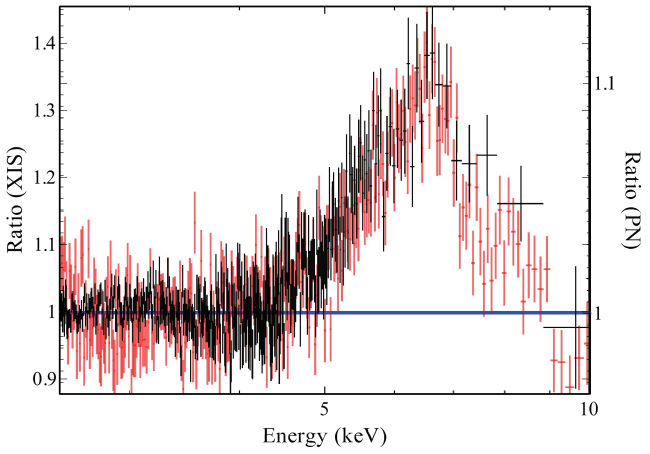

Figure 3. Close-up of the line profile for the *Suzaku* (black) and *XMM–Newton* (red) observations. It is clear that the line profile has varied very little between the observations. Note that the *XMM–Newton* observation has its own ratio scale shown on the right.

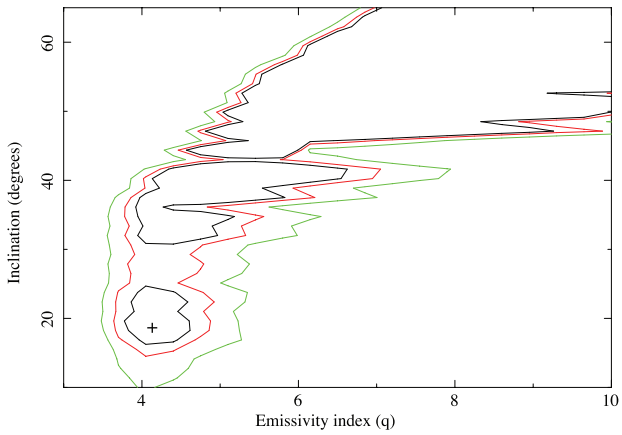

Figure 4. Inclination versus emissivity index contour plots for XTE J1752−223 (Model 1). The 68, 90 and 95 per cent confidence range for two parameters of interest are shown in black, red and green, respectively. The cross marks the position of the global minimum.

being consistent amongst the data sets at 2σ (green contour in Fig. 5).

Suzaku observations of the stellar mass black holes J1655−40 and Cyg X-1 in the low-hard state have suggested that the the broad-band continuum in this state has a more concave shape than that predicted by a single COMPPS component together with reflection (Makishima et al. 2008; Takahashi et al. 2008). To account for this effect the authors proposed a double-COMPPS model in line with previous double-Comptonization work (Gierlinski et al. 1997; Ibragimov et al. 2005). Such a model is suggestive of a system where the accretion disc is truncated and the Comptonization region is inhomogeneous (for a detailed description of this model and interpretation see Takahashi et al. 2008). In order to test whether such curvature in the continuum could result in a narrower line profile in the low-hard state observation of XTE J1752−223 we include an extra COMPPS component to Model 3. Similarly to the work of Makishima et al. (2008) we constrain both components to have the same seed photon and electron temperature, and the same reflection parameters, but allow them to differ in normalization and optical depth. The electron temperature could not be constrained and was thus frozen at 100 keV similarly to the value found for Cyg X-1. The presence of a strong and broad emission line (again modelled with the LAOR line profile) at 6.7 ± 0.1 keV remained none the less (see bottom panel of Fig. 2), with an EW of 130^{+20}_{-10} eV slightly lower than the values found for all other combinations for the continuum (see Table 1) as expected for such a curved continuum. However, this fit to the low-hard state data set ($\chi^2/\nu = 1162.8/1566$) still requires an accretion disc extending to within $3.9 \pm 0.5 r_{\rm g}$ of the central black hole.

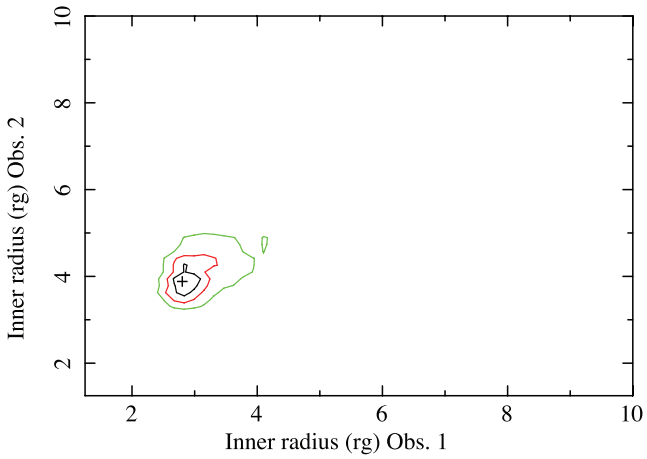

Figure 5. Contour plot showing the inner-edge radii for both the intermediate (Obs. 1) and low-hard state (Obs. 2) observations of XTE J1752−223. This provides explicit evidence that the radial extent of the accretion disc does not change between these states. As before the 68, 90 and 95 per cent confidence range for two parameters of interest are shown in black, red and green, respectively. The cross marks the position of the global minima.

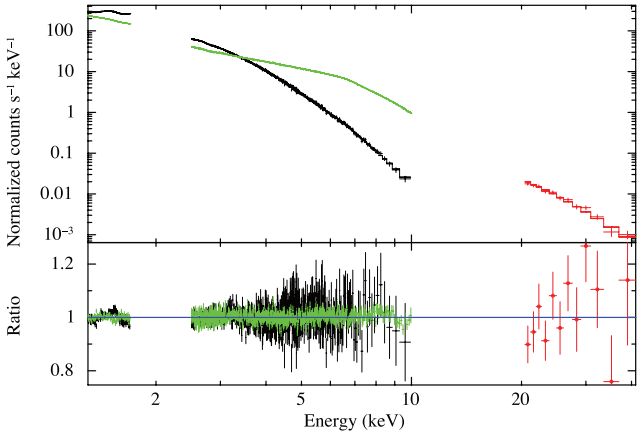

Figure 6. *Suzaku* and *XMM–Newton* spectra of XTE J1752−223 together with the ratio of the data to a model consisting of a self-consistent reflection component and a power law (Model 4). The spectra have been binned for visual clarity only. *Suzaku* XIS and PIN are shown in black and red, respectively. *XMM–Newton* EPIC-pn spectrum is shown in green.

3.2 Self-consistent disc reflection

In all our previous fits a broad iron emission line has been shown to be robustly present above a thermal-disc and power-law-like continuum. In this section we use the reflection model REFBHB developed by Ross & Fabian (2007) to self-consistently model both the thermal emission as well as the reflection features. Such analyses have previously been made for the stellar mass black hole in GX 339−4 and SWIFT J1753.5−0127 where it was shown that the black holes are rotating with a dimensionless spin parameter of approximately 0.93 ± 0.01 and 0.76 ± 0.15, respectively (Reis et al. 2008, 2009a). A current shortcoming of the reflection model is that it assumes a single-temperature accretion disc. However, in Reis et al. (2008) we showed that such an assumption does not have any significant effect on the inferred innermost radius of emission by (i) simulating a 'real' disc with known inner radius and comparing it with the measured value using REFBHB and (ii) comparing the results obtained with REFBHB with that of a thermal model (KERRBB; Li et al. 2005), which includes relativistic smearing in a disc with radial temperature gradient. In both cases there were no indication of any strong systematic variation in the values obtained from the single-temperature model possibly due to the the dominance of relativistic smearing over the intrinsic broadening due the nature of the multicolour disc. The parameters of the REFBHB model are the number density of hydrogen in the illuminated surface layer, $H_{\rm den}$, the temperature of the blackbody heating the surface layers, the power-law photon index, and the ratio of the total flux illuminating the disc to the total blackbody flux emitted by the disc. To be able to directly compare the results with that obtained with the simple models (Section 3.1), we start by convolving the reflection component with the relativistic blurring kernel KDBLUR, which is derived from the same code by Laor (1991). The power-law index of REFBHB is tied to that of the hard component and as before we constrain the inclination and inner disc radius to be the same between the observations. Note that we have now removed the upper-limit constraint on the inclination and allow the full parameter space to be explored. The model results in an excellent fit to the data with $\chi^2/\nu = 2579.3/2247$ (Model 4, see Fig. 6). The parameters are shown in Table 2. Fig. 7 shows the model for both the *Suzaku* intermediate state (left) and the *XMM–Newton* low-hard state (right) observations.

The results presented in Tables 1 and 2 suggest that the accretion disc in XTE J1752−223 extends down to within $3.7^{+0.6}_{-0.7} r_{\rm g}$ of the central black hole. This constraint can be better appreciated in Fig. 8, where the various confidences levels for $r_{\rm in}$ are shown as the dashed lines in the χ^2 plot. Also shown in Fig. 8 are the confidence levels for the value of $r_{\rm in}$ as obtained via the LAOR line profile (Model 1). It is clear that the inner radius found by modelling the line profile is consistent with that obtained from the physically motivated and self-consistent reflection model thus confirming the robustness of results obtained from line-profile fitting in stellar mass black holes, AGNs and neutron stars (stellar mass BH: Miller et al. 2002, 2004a, 2009a; Blum et al. 2009; Reis et al. 2009a; Hiemstra et al. 2010; AGNs: Fabian et al. 2002, 2009; Fabian & Vaughan 2003; Miniutti et al. 2009; Schmoll et al. 2009; Zoghbi et al. 2010; NS: Bhattacharyya & Strohmayer 2007; Cackett et al. 2008, 2009, 2010; di Salvo et al. 2009, Reis, Fabian & Young 2009b). Assuming that this radius is the same as the radius of marginal stability (Reynolds & Fabian 2008), our results implies that the black hole in XTE J1752−223 is rotating with an intermediate spin parameter. To test this we replaced the convolution model KDBLUR with the model KERRCONV (Brenneman & Reynolds 2006). This convolution model is a fully relativistic code which enables the black hole spin to be fit as a free parameter and does not assume specific spin a priori. The parameters for this fit are listed in Table 2 (Model 5). In this manner we find the spin of the black hole in XTE J1752−223 to be $a = 0.52^{+0.13}_{-0.16}$ at the 90 per cent confidence level (Fig. 9) and place a strong upper limit of $a \lesssim 0.7$ at greater than 5σ.

4 SUMMARY AND CONCLUSIONS

We have observed the black hole candidate XTE J1752−223 on two separate occasions during the decay of its 2009 outburst (Fig. 1). By fitting the energy spectra we found that the earlier, *Suzaku* observation caught the source in the intermediate state with a luminosity of approximately $0.2 L_{\rm Edd}$, whereas the subsequent *XMM–Newton* observation found it to be in the canonical low-hard state with $L/L_{\rm Edd} \approx 2 \times 10^{-2}$ assuming a 10 $M_{\odot}$ at a distance of 10 kpc. Both spectra shows the presence of a broad and asymmetric Fe emission line with EW decreasing from 270 to 170 eV. The line

Table 2. Joint fits with self-consistent reflection models.

	Model 4 kdblur*refbhb + power law		Model 5 kerrconv*refbhb + power law	
Parameters	Obs. 1	Obs. 2	Obs. 1	Obs. 2
$N_{\rm H}$ ($\times 10^{22}$ cm^{-2})	0.36 ± 0.01	0.34 ± 0.01	$0.37^{+0.01}_{-0.02}$	$0.36^{+0.05}_{-0.04}$
Γ	$2.53^{+0.08}_{-0.09}$	1.83 ± 0.02	$2.54^{+0.02}_{-0.11}$	1.83 ± 0.02
$T_{\rm disc}$ (keV)	$0.47^{+0.02}_{-0.01}$	$0.30^{+0.01}$	0.47 ± 0.01	0.305 ± 0.005
$F_{\rm Illum}/F_{\rm BB}$	$0.3^{+0.2}_{-0.1}$	$4.0^{+0.1}_{-0.2}$	$0.28^{+0.05}_{-0.08}$	$3.94^{+0.13}_{-0.15}$
$H_{\rm den}$ ($\times 10^{20}$)	$0.22^{+0.06}_{-0.07}$	$25.8^{+3.7}_{-3.0}$	$0.22^{+0.06}_{-0.02}$	26^{+3}_{-2}
$N_{\rm Refbhb}$ ($\times 10^{-2}$)	44^{+16}_{-19}	$4.4^{+0.8}_{-0.7}$	45^{+5}_{-1}	$4.5^{+0.2}_{-0.4}$
$N_{\rm hard}$	$0.12^{+0.12}_{-0.11}$	0.24 ± 0.01	$0.13^{+0.04}_{-0.13}$	0.24 ± 0.01
q	$3.6^{+1.4}_{-0.5}$	$2.4^{+0.2}_{-0.1}$	$4.0^{+1.1}_{-0.4}$	2.5 ± 0.1
θ (°)	25^{+7}_{-8}	=Obs. 1	28^{+4}_{-8}	=Obs. 1
$r_{\rm in}$ ($r_{\rm g}$)	$3.7^{+0.6}_{-0.7}$	=Obs. 1	–	–
Spin (a)	–	–	$0.52^{+0.13}_{-0.16}$	=Obs. 1
χ^2/ν	2579.3/2247		2580.2/2247	

Note: Results of joint *Suzaku* (Obs. 1) and *XMM–Newton* (Obs. 2) fits with the self-consistent reflection model REFBHB. In all cases the inclination, inner disc radii (or spin) were tied between the observations. Model 4 uses the kernel from the LAOR line profile to account for the gravitational effects close to the black hole. Model 5 replaces KDBLUR with the fully relativistic code KERRCONV were the spin is a parameter of the model. In both cases the hard emission illuminating the disc is assumed to be a power law with index Γ. All errors are 90 per cent confidence for one parameter.

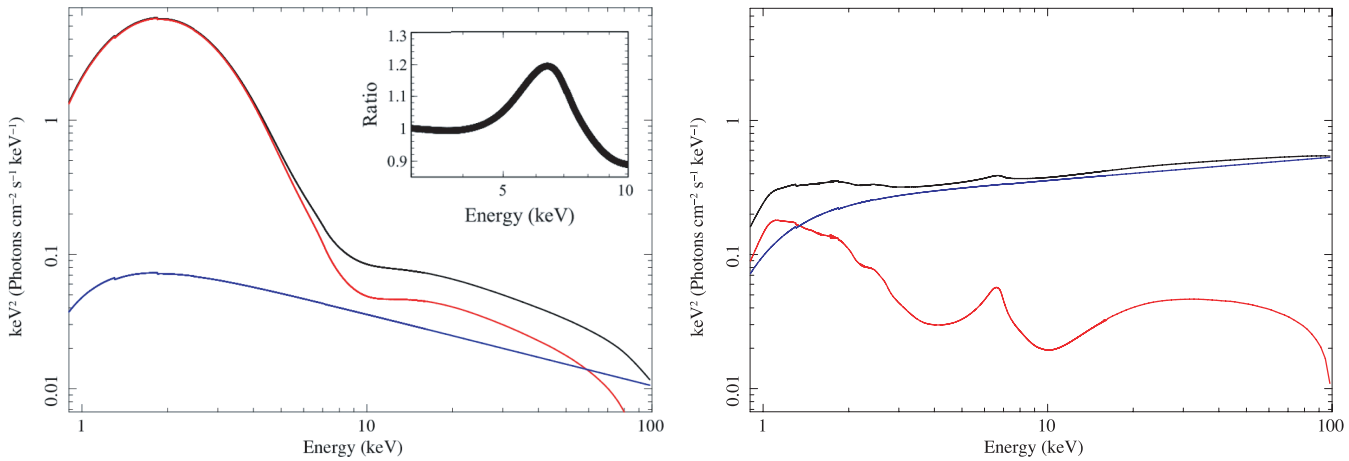

Figure 7. Best-fitting model for the *Suzaku* spectrum of XTE J1752−223 in the intermediate state (left) and *XMM–Newton* spectrum in the low-hard state (right). The total model is shown in black, with the power law and REFBHB components shown in blue and red, respectively. The inset in the left-hand panel show the line profile obtained by dividing the current model with the best-fitting power law plus DISKBB continuum.

profile is found to be remarkably similar between the two states (Fig. 3) and robust to a variety of continua (Fig. 2). Furthermore we find that a thermal disc component is required in both states with the variation in flux following closely the $L \propto T^4$ relation. The requirement of both a thermal disc component as well as a strong (EW $>$ 150 eV) and asymmetric Fe emission line in the low-hard adhere to the strong observational criteria described in Reis, Fabian & Miller (2010) and is further evidence that the accretion disc does not begin to recede at the onset of the low-hard state. Our result is in direct contrast with the truncated disc paradigm which suggest that the disc recedes at the outset of the low-hard state and is thereby replaced by advection or magnetically dominated accretion flows.

By modelling the full reflection features present in the spectra of XTE J1752−223 with a self-consistent reflection model, we have shown in Fig. 8 that the inner disc extends down to $3.7^{+0.6}_{-0.7} r_{\rm g}$ at the 90 per cent level of confidence. Such a joint fit to the multiple states with a common model allows for the explicit treatment of variations in the ionization and/or structure of the accretion disc while at the same time reducing the errors on intrinsic physical parameters such as the inner-disc inclination and black hole spin (Miller et al. 2008; Reis et al. 2008; Miller et al. 2009a). We note also that similar values for $r_{\rm in}$ are found when fitting the Fe Kα line profile with a variety of phenomenological models, thus confirming the robustness of inner radii measurements via such reflection features. By using a fully relativistic convolution code (KERRCONV) acting on a self-consistent reflection model (REFBHB), we formally constrained the spin of the black hole in XTE J1752−223 to be $a = 0.52^{+0.13}_{-0.16}$ at the 90 per cent level of confidence, thus ruling out a non-rotating, Schwarzschild black hole at greater than the 3σ confidence level and a maximally rotating black hole at more than the 9σ level of confidence (Fig. 9).

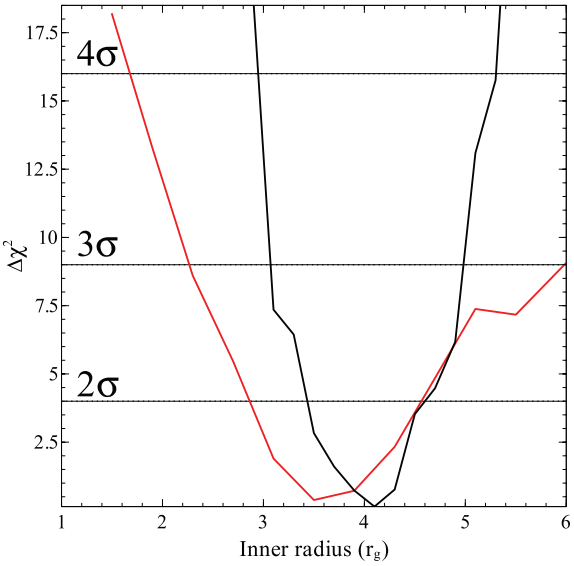

Figure 8. Goodness-of-fit versus inner radius for Model 1 (black) and Model 4 (red). The inner radii measured with these two distinct models are found to be consistent with each other. Taking the value obtained for the physically consistent model (Model 4; red) as a conservative indication of the inner extent of the accretion disc we find $r_{\rm in}$ to be $3.7^{+0.6}_{-0.7} r_{\rm g}$ at the 90 per cent confidence level ($\Delta\chi^2 = 2.71$ for one parameter of interest). The dotted lines indicate confidence intervals.

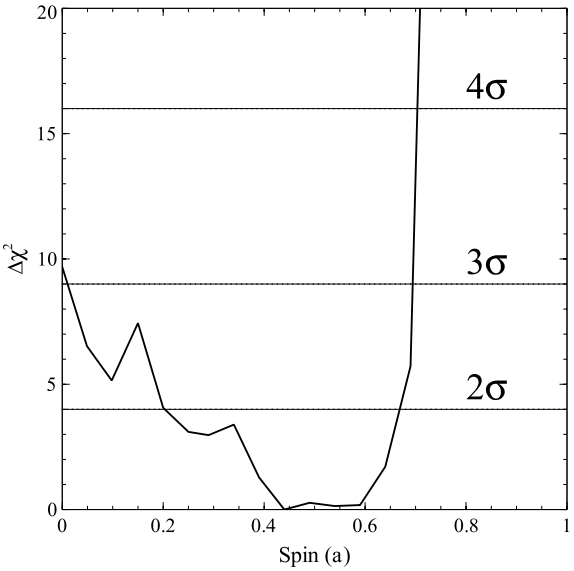

Figure 9. Goodness-of-fit versus spin for Model 5. It is clear that the black hole in XTE J1752−223 is not maximally rotating, with a spin of $a = 0.998$ being excluded at over 9σ. A non-rotating, Schwarzschild black is excluded at the 3σ level of confidence.

The clear spectral differences between the two states (see Fig. 7) can potentially be ascribed to physical changes in the disc properties. In the intermediate state the disc contributes mostly towards the heating of the atmosphere whereas in the low-hard state this is achieved mostly by flux from the Comptonizing region (see Table 2). This difference is partially due to the much lower thermal flux in the low-hard state, but it may also reflect an increase in the accretion power being funnelled into the corona or jet. The increase in hydrogen number density in the low-hard state as compared to the intermediate state, together with the lack of radial variation in the disc is likely attributed to changes in the atmosphere of the inner disc indicating that the disc is more vertically extended in the intermediate state. Changes in the physical properties of the inner disc has previously been proposed as viable alternative to disc truncation (Merloni, Fabian & Ross 2000) and has recently been invoked to partly explain the variable behaviour of GX 339−4 in the low-hard state (Wilkinson & Uttley 2009). The decrease in the EW of the iron Kα line between the states is characteristic of a decrease in the reflection fraction (R; George & Fabian 1991). This behaviour is usually seen in stellar mass black holes and can be explained without invoking disc truncation by assuming that either the inner disc becomes fully ionized (Ross, Fabian & Young 1999) or/and that the corona is moving relativistically away from the disc (Beloborodov 1999).

The natal spin of a stellar mass black holes produced via single collapse events is often thought to be be $\lesssim$0.75–0.9 depending on the type of the SN or GRB that preceded its formation and the physical structure (magnetic field, angular momentum, metallicity, etc.) of the progenitor star (see e.g. Heger & Woosley 2002; Shibata & Shapiro 2002; Gammie et al. 2004). However, subsequent accretion process has been shown to spin-up the central black hole to values >0.9 (Gammie et al. 2004; Volonteri et al. 2005) under certain conditions. The intermediate value for the spin parameter found here suggest that the black hole in XTE J1752−223 has not changed its natal spin by a significant amount.

ACKNOWLEDGMENTS

RCR would like to thank the anonymous referee and the Science and Technology Research Council (STFC). ACF thanks the Royal Society. EMC and CSR gratefully acknowledge support provided by NASA through the Chandra Fellowship Programme and the US National Science Foundation under grant AST 06-07428, respectively.

REFERENCES

Anders E., Grevesse N., 1989, Geochimica Cosmochimica Acta, 53, 197
Balucinska-Church M., McCammon D., 1992, ApJ, 400, 699
Beloborodov A. M., 1999, ApJ, 510, L123
Bhattacharyya S., Strohmayer T. E., 2007, ApJ, 664, L103
Blum J. L., Miller J. M., Fabian A. C., Miller M. C., Homan J., van der Klis M., Cackett E. M., Reis R. C., 2009, ApJ, 706, 60
Boldt E., 1987, in Hewitt A., Burbidge G., Fang L. Z., eds, Proc. IAU Symp. 124, Observational Cosmology. Kluwer, Dordrecht, p. 611
Brenneman L. W., Reynolds C. S., 2006, ApJ, 652, 1028
Brocksopp C., Corbel S., Tzioumis T., Fender R., 2009, Astron. Telegram, 2278, 1
Cackett E. M. et al., 2008, ApJ, 674, 415
Cackett E. M., Altamirano D., Patruno A., Miller J. M., Reynolds M., Linares M., Wijnands R., 2009a, ApJ, 694, L21
Cackett E. M. et al., 2010, ApJ, 720, 205C
Dickey J. M., Lockman F. J., 1990, ARA&A, 28, 215
di Salvo T. et al., 2009, MNRAS, 398, 2022
Fabian A. C., Vaughan S., 2003, MNRAS, 340, L28
Fabian A. C., Rees M. J., Stella L., White N. E., 1989, MNRAS, 238, 729
Fabian A. C., Nandra K., Reynolds C. S., Brandt W. N., Otani C., Tanaka Y., Inoue H., Iwasawa K., 1995, MNRAS, 277, L11
Fabian A. C. et al., 2002, MNRAS, 335, L1
Fabian A. C. et al., 2009, Nat, 459, 540
Fender R. P., Belloni T. M., Gallo E., 2004, MNRAS, 355, 1105
Frank J., King A., Raine D. J., 2002, Accretion Power in Astrophysics, 3rd edn. Cambridge Univ. Press, Cambridge
Gammie C. F., Shapiro S. L., McKinney J. C., 2004, ApJ, 602, 312

George I. M., Fabian A. C., 1991, MNRAS, 249, 352
Gierlinski M., Zdziarski A. A., Done C., Johnson W. N., Ebisawa K., Ueda Y., Haardt F., Phlips B. F., 1997, MNRAS, 288, 958
Gou L. et al., 2009, ApJ, 701, 1076
Heger A., Woosley S. E., 2002, ApJ, 567, 532
Hiemstra B., Mendez M., Done C., Diaz Trigo M., Altamirano D., Casella P., 2010, arXiv e-prints
Ibragimov A., Poutanen J., Gilfanov M., Zdziarski A. A., Shrader C. R., 2005, MNRAS, 362, 1435
Jansen F. et al., 2001, A&A, 365, L1
Koyama K. et al., 2007, PASJ, 59, 23
Laor A., 1991, ApJ, 376, 90
Li L., Zimmerman E. R., Narayan R., McClintock J. E., 2005, ApJS, 157, 335
McClintock J. E., Shafee R., Narayan R., Remillard R. A., Davis S. W., Li L., 2006, ApJ, 652, 518
Makishima K., Maejima Y., Mitsuda K., Bradt H. V., Remillard R. A., Tuohy I. R., Hoshi R., Nakagawa M., 1986, ApJ, 308, 635
Makishima K. et al., 2008, PASJ, 60, 585
Markwardt C. B. et al., 2009a, Astron. Telegram, 2258, 1
Markwardt C. B., Barthelmy S. D., Evans P. A., Swank J. H., 2009b, Astron. Telegram, 2261, 1
Martocchia A., Matt G., Karas V., Belloni T., Feroci M., 2002, A&A, 387, 215
Merloni A., Fabian A. C., Ross R. R., 2000, MNRAS, 313, 193
Miller J. M., 2007, ARA&A, 45, 441
Miller J. M. et al., 2002, ApJ, 570, L69
Miller J. M. et al., 2004a, ApJ, 606, L131
Miller J. M. et al., 2004b, ApJ, 601, 450
Miller J. M. et al., 2008, ApJ, 679, L113
Miller J. M., Reynolds C. S., Fabian A. C., Miniutti G., Gallo L. C., 2009a, ApJ, 697, 900
Miller J. M., Cackett E. M., Reis R. C., 2009b, ApJ, 707, L77
Miniutti G., Panessa F., de Rosa A., Fabian A. C., Malizia A., Molina M., Miller J. M., Vaughan S., 2009, MNRAS, 398, 255
Mitsuda K. et al., 1984, PASJ, 36, 741
Mitsuda K. et al., 2007, PASJ, 59, 1
Nakahira S. et al., 2009, Astron. Telegram, 2259, 1
Nakahira S. et al., 2010, PASJ, arXiv:1007.0801
Poutanen J., Svensson R., 1996, ApJ, 470, 249
Reis R. C., Fabian A. C., Ross R. R., Miniutti G., Miller J. M., Reynolds C., 2008, MNRAS, 387, 1489
Reis R. C., Fabian A. C., Ross R. R., Miller J. M., 2009a, MNRAS, 395, 1257
Reis R. C., Fabian A. C., Young A. J., 2009b, MNRAS, 399, L1
Reis R. C., Fabian A. C., Miller J. M., 2010, MNRAS, 402, 836
Remillard R. A., McClintock J. E., 2006, ARA&A, 44, 49
Reynolds C. S., Fabian A. C., 2008, ApJ, 675, 1048
Reynolds C. S., Nowak M. A., 2003, Phys. Rep., 377, 389
Reynolds C. S., Wilms J., 2000, ApJ, 533, 821
Ross R. R., Fabian A. C., 2005, MNRAS, 358, 211
Ross R. R., Fabian A. C., 2007, MNRAS, 381, 1697
Ross R. R., Fabian A. C., Young A. J., 1999, MNRAS, 306, 461
Schmoll S. et al., 2009, ApJ, 703, 2171
Shafee R., McClintock J. E., Narayan R., Davis S. W., Li L., Remillard R. A., 2006, ApJ, 636, L113
Shakura N. I., Sunyaev R. A., 1973, A&A, 24, 337
Shibata M., Shapiro S. L., 2002, ApJ, 572, L39
Strüder L. et al., 2001, A&A, 365, L18
Takahashi T. et al., 2007, PASJ, 59, 35
Takahashi H. et al., 2008, PASJ, 60, 69
Thorne K. S., 1974, ApJ, 191, 507
Titarchuk L., 1994, ApJ, 434, 570
Tomsick J. A., Yamaoka K., Corbel S., Kaaret P., Kalemci E., Migliari S., 2009, ApJ, 707, L87
Torres M. A. P., Jonker P. G., Steeghs D., Yan H., Huang J., Soderberg A. M., 2009a, Astron. Telegram, 2263, 1
Torres M. A. P., Steeghs D., Jonker P. G., Thompson I., Soderberg A. M., 2009b, Astron. Telegram, 2268, 1
Turner M. J. L. et al., 2001, A&A, 365, L27
Uchiyama Y. et al., 2008, PASJ, 60, 35
Volonteri M., Madau P., Quataert E., Rees M. J., 2005, ApJ, 620, 69
Wilkinson T., Uttley P., 2009, MNRAS, 397, 666
Wilson-Hodge C. A., Camero-Arranz A., Case G., Chaplin V., Connaughton V., 2009, Astron. Telegram, 2280, 1
Zoghbi A., Fabian A. C., Uttley P., Miniutti G., Gallo L. C., Reynolds C. S., Miller J. M., Ponti G., 2010, MNRAS, 401, 2419

This paper has been typeset from a TEX/LATEX file prepared by the author.